J. Membrane Biol. 195, 93–108 (2003)
DOI: 10.1007/s00232-003-2048-2

The Journal of
Membrane
Biology

Identification of Ion-Selectivity Determinants in Heavy-Metal Transport P_{1B}-type ATPases

J.M. Argüello
Department of Chemistry and Biochemistry, Worcester Polytechnic Institute, 100 Institute Rd., Worcester, MA 01609, USA

Received: 3 April 2003/Revised: 30 June 2003

Abstract. P_{1B}-type ATPases transport a variety of metals (Cd^{2+}, Zn^{2+}, Pb^{2+}, Co^{2+}, Cu^{2+}, Ag^{+}, Cu^{+}) across biomembranes. Characteristic sequences CP[C/H/S] in transmembrane fragment H6 were observed in the putative transporting metal site of the founding members of this subfamily (initially named CPx-ATPases). In spite of their importance for metal homeostasis and biotolerance, their mechanisms of ion selectivity are not understood. Studies of better-characterized P_{II}-type ATPases (Ca-ATPase and Na,K-ATPase) have identified three transmembrane segments that participate in ion binding and transport. Testing the hypothesis that metal specificity is determined by conserved amino acids located in the equivalent transmembrane segments of P_{1B}-type ATPases (H6, H7, and H8), 234 P_{1B}-ATPase protein sequences were analyzed. This showed that although H6 contains characteristic CPX or XPC sequences, conserved amino acids in H7 and H8 provide signature sequences that predict the metal selectivity in each of five P_{1B}-ATPase subgroups identified. These invariant amino acids contain diverse side chains (thiol, hydroxyl, carbonyl, amide, imidazolium) that can participate in transient metal coordination during transport and consequently determine the particular metal selectivity of each enzyme. Each subgroup shares additional structural characteristics such as the presence (or absence) of particular amino-terminal metal-binding domains and the number of putative transmembrane segments. These differences suggest unique functional characteristics for each subgroup in addition to their particular metal specificity.

Key words: P-type ATPase — CPx-ATPase — Cu-ATPase — Metal binding site — Zinc — Cadmium — Cobalt — Copper — Silver — CopA — CadA — ZntA — CopB

Introduction

P_{1B}-type ATPases belong to the large P-type ATPase family of membrane proteins. These enzymes transport ions against their concentration gradients, using the energy provided by ATP hydrolysis. Comparison of primary sequences, proposed topological arrangements and ion specificity have allowed the organization of the P-type ATPases into five subfamilies (I, II, III, IV and V) (Axelsen & Palmgren, 1998). The P_{II} group includes the Na,K-ATPase, plant and yeast H-ATPases, and sarcoplasmic reticulum (SR[1]) Ca-ATPase, among others. These enzymes have been extensively studied and have provided the current experimental framework to describe the mechanism of ion transport by all P-type ATPases (Glynn, 1985; Pedersen & Carafoli, 1987; Axelsen & Palmgren, 1998). Within this mechanism, the catalytic phosphorylation of the aspartyl group in the consensus sequence DKTGT is the unifying characteristic of all P-type ATPases.

P_{1B}-type ATPases transport heavy metals (Cd^{2+}, Zn^{2+}, Pb^{2+}, Co^{2+}, Cu^{2+}, Ag^{+}, Cu^{+}) across biomembranes, playing a key role in the homeostasis and mechanisms of biotolerance of these metals (Vulpe & Packman, 1995; Solioz & Vulpe, 1996; Rensing, Ghosh & Rosen, 1999). Their relevance is evident when considering that mutations of the two human Cu^{+}-ATPases are responsible for Menkes and Wilson diseases (Bull et al., 1993; Bull & Cox, 1994; Vulpe & Packman, 1995). Similarly, the abundance of P_{1B}-ATPases in plants (eight genes in the *Arabidopsis thaliana* genome) speaks of fundamental and complex roles for these proteins in plant micronutrient metal metabolism (Hirayama et al., 1999; Williams, Pittman & Hall, 2000; Woeste & Kieber, 2000).

The enzymatic and transport properties have been established for some P_{1B}-ATPases (Tsai, Yoon &

Correspondence to: arguello@wpi.edu

[1] *Abbreviations*: SR, sarcoplasmic reticulum; TMs, transmembrane segments; N-MBD, N-terminal metal binding domain.

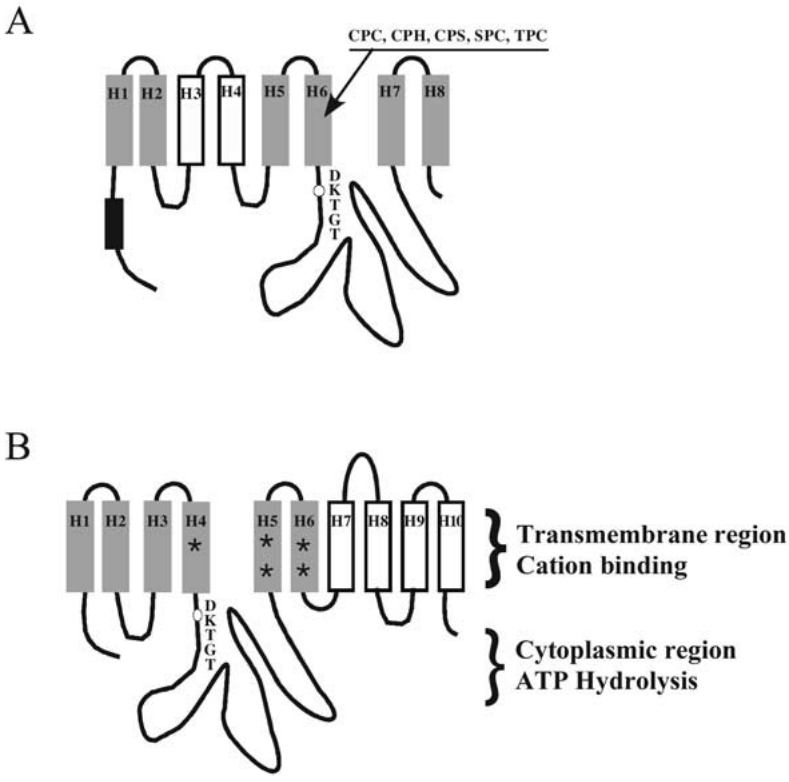

Fig. 1. Scheme representing the membrane topology of a typical P_{1B}-type ATPase (*A*) and a P_{II}-type ATPase (*B*). H1–10 represent transmembrane segments. Dark grey transmembrane segments are assumed structurally equivalent. White transmembrane segments are distinct for each subgroup, black block represents N-terminal metal-binding domains, * indicates amino acids identified in the SR Ca-ATPase and in the Na,K-ATPase as involved in cation coordination. DKTGT is the consensus distinctive of the catalytic phosphorylation site. CPC, CPH, SPC, TPC, and CPS are sequences characteristic of the transmembrane metal-binding site of P_{1B}-ATPases.

Lynn, 1992; Odermatt et al., 1993; Tsai & Linet, 1993; Phung, Ajlani & Haselkorn, 1994; Solioz & Odermatt, 1995; Rensing, Mitra & Rosen, 1997; Voskoboinik et al., 1988; La Fontaine et al., 1999; Okkeri & Haltia, 1999; Rutherford, Cavet & Robinson, 1999; Rensing et al., 2000; Sharma et al., 2000). All tested enzymes drive the export of ions out of cells. Two reports have shown that removal of CopA gene from *E. hirae* (P32113[2]) (Odermatt et al., 1993) or the homologous gene in *Synechococcus* PCC7942 (P37385) (Phung et al., 1994) allows cells to grow in high extracellular Cu^{2+} and proposed a consequent role in metal influx for these enzymes. However, biochemical studies of homologous enzymes from *E. coli* (Q59385) (Rensing et al., 2000; Fan & Rosen, 2002) and *A. fulgidus* (O29777) (Mandal et al., 2002) have indicated that these are Cu^{+}-exporting enzymes. Functional assays (transport, ATPase activation, metal dependence of phosphoenzyme formation and stability) have shown that Ag^{+} can also activate Cu^{+}-ATPases (Solioz & Odermatt, 1995; Rensing et al., 2000; Fan & Rosen, 2002; Mandal et al., 2002). Similarly, Zn^{2+}-ATPases can use Cd^{2+} or Pb^{2+} as substrates (Tsai et al., 1992; Rensing et al., 1997; Okkeri & Haltia, 1999; Sharma et al., 2000), while the *A. fulgidus* CopB (O30085) is activated by Cu^{2+}, Cu^{+} and Ag^{+} (Argüello, Mandal & Mana-Capelli, 2003). Only one of the tested P_{1B}-ATPases, *Synechocystis* PCC6803 CoaT (Q59997), seems to be involved in Co^{2+} transport (Rutherford et al., 1999). Disruption of CoaT reduced Co^{2+} tolerance and increased cytoplasmic Co^{2+} accumulation.

Based on hydrophobicity analysis previous studies have suggested that most P_{1B}-ATPases appear to have eight transmembrane segments (TMs) (Fig. 1*A*) (Bull & Cox, 1994; Lutsenko & Kaplan, 1995; Solioz & Vulpe, 1996; Axelsen & Palmgren, 1998, 2001). This membrane topology has been experimentally confirmed for CadA from *H. pylori* (Q59465) (Melchers et al., 1996) and *S. aureus* (Plasmid pI258) CadA (P20021) (Tsai et al., 2002). In early studies two other structural characteristics allowed the identification of available P_{1B}-ATPase sequences: a) the signature sequence (CPC, CPH, CPS) present in their sixth TM (H6) (additional sequences now also show SPC and TPC at this TM; thus the misnomer of these enzymes as CPx-ATPases); and b) one or more ion metal binding domains in the cytoplasmic N-terminal region (N-MBD) (Bull & Cox, 1994; Lutsenko & Kaplan, 1995; Solioz & Vulpe, 1996; Jordan et al., 2001) (Fig. 1*A*).

Experimental evidence supports the early idea that conserved Cys in H6 participate in metal binding and transport (Bull & Cox, 1994; Lutsenko & Kaplan, 1995; Solioz & Vulpe, 1996; Axelsen & Palmgren, 1998; Rensing et al., 1999). Mutation of

[2]All accession numbers starting with a letters O, P and Q are from the SWISS-PROT database. Those starting with letters A, B, E, N and Z are from GenBank. Whenever available the SWISS-PROT number has been used.

CPC → CPA in the *C. elegans* Cu-ATPase (O17737) yielded a protein unable to rescue a Cu-ATPase (P38995)-deficient yeast mutant (Δ*ccc2*) (Yoshimizu et al., 1998). Similar results were observed when mutation CPH → SPH was introduced in *E. hirae* CopB (P05425) (Bissig et al., 2001). Replacement of Cys in the CPC of *E. coli* CopA (Q59385), a Cu^+-ATPase, resulted in loss of copper resistance, transport and phosphoenzyme formation (Fan & Rosen, 2002). We have observed that similar replacements in *A. fulgidus* CopA (O2977) produce enzymes able to bind the nucleotide but unable to phosphorylate in the presence of Cu^+ and ATP (Mandal and Argüello, unpublished results). Thus, these results corroborate that the CPC sequence is essential for enzyme function. However, a point that is still not understood is the relationship between ion specificity and the various sequences in H6 (CPC, CPH, SPC, TPC or CPS). Does each of these sequences confer a different selectivity? On the other hand, it is puzzling that different enzymes carrying the CPC sequence in H6 transport either monovalent (Cu^+, Ag^+) or divalent (Zn^{2+}, Cd^{2+}, Pb^{2+}) metals (Tsai et al., 1992; Rensing et al., 1997; Yoshimizu et al., 1998; Okkeri & Haltia, 1999; Voskoboinik et al., 1999; Rensing et al., 2000; Sharma et al., 2000; Fan & Rosen, 2002; Mandal et al., 2002). This question can be answered by identifying the consensus sequences truly specific for each particular selectivity. In turn, this information would allow us not only to predict the transported ion but also begin to understand the principles governing transient heavy metal binding by transport proteins.

Ion transport by membrane proteins likely involves the transient coordination of the ion by an appropriate number of polypeptide backbone or amino-acid side-chain atoms (electronegative Lewis bases in the case of transition metals) (Cowan, 1996; Toyoshima et al., 2000; Fraústro da Silva & Williams, 2001; Zhou et al., 2001; Dutzler et al., 2002; Toyoshima & Nomura, 2002). Consequently, the specific atoms participating in this coordination and the geometry of their arrangement would determine the transported ion, i.e., the protein selectivity. Similarly, it could be expected that these structural characteristics would be maintained in members of a given transport family having the same ion specificity. In the case of P_{1B}-ATPases, it can be hypothesized that side chains in the conserved sequences in H6 would participate in metal coordination. However, it is unlikely that these are the only selectivity determinants since enzymes with the CPC sequence transport different metals (either Cu^+/Ag^+ or $Zn^{2+}/Cd^{2+}/Pb^{2+}$). It can also be considered that the metal binding sites should support the conformational transitions associated with metal translocation and experience a reduction in affinity necessary for metal release to the opposite side of the permeability barrier. These are likely achieved by the participation of coordinating atoms in different TMs that undergo key movements during transport. Assuming that both P_{II} and P_{1B}-type ATPases share a common core structure responsible for essential aspects of their function, a starting point to identify metal-coordinating amino-acid side-chains is to compare the structural-functional characteristics of P_{1B}-ATPases to those of the better-characterized P_{II}-ATPases. Recently, the structure of the Ca^{2+}-bound SR Ca-ATPase was reported (Toyoshima et al., 2000; Ogawa & Toyoshima, 2002). This structure, together with structural-functional studies of the SR Ca-ATPase and the Na,K-ATPase, has shown that amino acids in their TMs H4, H5 and H6 are responsible for ion binding during transport (Argüello & Kaplan, 1994; Argüello & Lingrel, 1995; Argüello et al., 1996, 1999; Kuntzweiler, Argüello & Lingrel, 1996; Pedersen et al., 1997; MacLennan et al., 1998; Pedersen et al., 1998; Vilsen & Andersen, 1998; Toyoshima et al., 2000) (Fig. 1*B*). Alignment of sequences and homology models suggest that TMs H6, H7 and H8 of P_{1B}-ATPases are structurally equivalent to H4, H5 and H6, respectively, of the P_{II} ATPases (Lutsenko & Kaplan, 1995; Palmgren & Axelsen, 1998; Sweadner & Donnet, 2001) (Fig. 1). Therefore, by homology with the P_{II}-ATPases, H6, H7 and H8 of P_{1B}-ATPases should participate in metal binding and transport, with key residues conserved among those enzymes with identical ion selectivity. Toward testing this hypothesis, all available P_{1B}-ATPase protein sequences were analyzed, searching for similarities and conserved residues in H6, H7, and H8. This approach allowed the identification of P_{1B}-ATPases subgroups where conserved residues appear to be signature sequences that correlate with particular metal specificities. The resulting signature sequences permit prediction of those enzymes that will transport Cu^+/Ag^+, $Cu^{2+}/Cu^+/Ag^+$, $Zn^{2+}/Cd^{2+}/Pb^{2+}$ or Co^{2+}, while also anticipate the existence of proteins with distinct metal specificity still to be determined. Furthermore, this survey revealed additional structural features that characterize each subgroup of P_{1B}-ATPases.

Materials and Methods

Most P_{1B}-ATPase protein sequences were obtained from the P-type ATPases database developed by Palmgren and Axelsen (http://biobase.dk/~axe/Patbase.html). Sequences were also identified by performing standard protein-protein BLAST [blastp] searches in the NCBI database (Altschul et al., 1990). Sequences of two particular regions of a given P_{1B}-ATPase (with a gap of indeterminate length between them) were used in these searches. Each region pair included: a) H6 and the downstream sequence extending until DKTGT (the consensus sequence that includes the Asp phosphorylated during the catalytic cycle of P-type ATPases), and b) the segments corresponding to putative H7 and H8. These TMs were identified by hydropathy

profile (*see* below). Each pair was taken from a typical member of each P_{1B}-ATPase subgroup identified in initial alignments, using sequences from the P-type ATPases database. These sequence pairs were: 1) Ser992-Thr1048 and Lys1353-Lys1408 from *H. sapiens* ATP7A/MNK (Q04656) (Menkes protein); 2) Gly385-Thr442 and N685-Leu729 from *S. typhi* P_{1B}-ATPase (Q8Z255); 3) Ala333-Leu395 and Q639-Ala686 from *A. fulgidus* CopB (O30085); and 4) Val287-Thr341 and Phe616-Leu633 from *B. subtilis* P_{1B}-ATPase (O31688). Finally, additional sequences were obtained by scanning the SWISS-PROT, TrEMBL, and TrEMBL-New databases with the ScanProsite online tool using the following patterns identified in the H7-H8 region of P_{1B}-ATPases: NX(6)YNX(4)PX(5,25)PX(6)MXX SSX(5)[NS], NX(7)KX(9)GX(5,15)DXG{EDKRP}(7)N, NX(5) GYNX(4)PX(10,20)PX(6)MSXSTX(5)N, and HEG[GS]TX(5)[NS] [GSA] (Gattiker, Gasteiger & Bairoch, 2002). This screening of databases revealed 234 full-length P_{1B}-ATPase sequences. Sequences from different strains of an organism were included in the data set only when they presented mutations in the TMs under study.

Sequences were aligned using commercial software (LaserGene, DNASTAR, Madison, WI) by Clustal W method (Thompson, Higgins & Gibson, 1994). The putative membrane topology of indicated P_{1B}-ATPases was obtained using the TMHMM 2.0 online server for prediction of transmembrane helices in proteins (Sonnhammer, von Heijne & Krogh, 1998). The phylogenetic tree of P_{1B}-ATPases was drawn with the DRAWTREE software from the PHYLIP package (Felsenstein, 1989).

Results

The goal of this analysis was to identify amino acids that probably participate in metal coordination during transport by P_{1B}-ATPases and consequent signature sequences that predict their metal specificity. 234 P_{1B}-ATPase protein sequences were obtained from the P-type ATPase database (http://biobase.dk/~axe/Patbase.html) and as result of various database searches using the regions of interest (H6, H7 and H8) (Tables 1, 2, 3, 4 and 5). All the obtained sequences showed the structural characteristics of P_{1B}-ATPases: the DKTGT phosphorylation site, either a CPC, CPH, SPC, CPS, or TPC sequence in H6 (two proteins with APC sequence were also identified) and no more than eight putative TMs. All sequences were closely related and 35% was the minimum Percent Identity observed.

The central hypothesis driving this P_{1B}-ATPase sequence analysis is that by analogy with the P_{II}-type ATPases, amino acids in TMs H6, H7 and H8 should be involved in metal transport by P_{1B}-ATPases and consequently be conserved in enzymes with identical metal specificity. Thus, sequences encoding for H6 and H7-H8 were separately analyzed and the P_{1B}-ATPases sorted in six subgroups with conserved sequences in these TMs. 140 sequences in Subgroup IB-1 and 47 in IB-2 have CPC in H6 (analysis of sequences in H7 and H8 allowed the differentiation in two groups, IB-1 and IB-2, with different invariant residues in this region); 16 in Subgroup IB-3 contain CPH; 21 in Subgroup IB-4 have SPC; and 5 in Subgroup IB-5 have TPC. Five sequences could not be arranged within this classification, although based on their overall similarity to other members of this subfamily (up to 45%) they appear to be P_{1B}-ATPases. These sequences were pooled in subgroup IB-6.

Structural-Functional Characteristics of subgroup IB-1

Proteins included in subgroup IB-1 are listed in Table 1. The large subgroup IB-1 includes some of the better characterized P_{1B}-ATPases such as the Menkes (Q04656) and Wilson (P35670) disease proteins (Bull et al., 1993; Bull & Cox, 1994; Petrukhin et al., 1994; Vulpe & Packman, 1995), *Arabidopsis thaliana* RAN1 (Q9S7J8) (Hirayama et al., 1999; Woeste & Kieber, 2000), *E. coli* CopA (Q59385) (Rensing et al., 2000; Fan & Rosen, 2002) and *A. fulgidus* CopA (O29777) (Mandal et al., 2002). Proteins belonging to this subgroup are found in archaea, prokaryotes and eukaryotes. Enzymatic and transport assays suggest that these are Cu^+-ATPases that drive the efflux of Cu^+ from the cytoplasm (Voskoboinik et al., 1999; Rensing et al., 2000; Fan & Rosen, 2002; Mandal et al., 2002). In those cases where metal selectivity has been tested, they are also activated by Ag^+ but not by divalent metals (Rensing et al., 2000; Fan & Rosen, 2002; Mandal et al., 2002).

Proteins in subgroup IB-1 are very diverse in length (from 650 to 1500 amino acids) due to the presence of a number (0–6) of metal-binding domains in their N-terminal end (*see* below). They all appear to have eight TMs with a large cytoplasmic loop between TMs H6 and H7. Figure 2 shows the sequence alignment of ten typical members of subgroup IB-1 in the regions of interest: a) H6 and the downstream sequence until the catalytic phosphorylation site, and b) the TMs H7 and H8 together with their joining loop. Note that in this and subsequent presentations of sequence alignments only ten sequences are shown; however, highlighted residues are conserved in all members of the corresponding subgroup. All sequences in subgroup IB-1 showed the invariant $CPC(X)_6P$ sequence in H6. No other residues are fully conserved although the ALGLAT sequence, between CPC and the Pro in the cytoplasmic end of H6, is conserved in more than 80% of these proteins. It is clear from the consensus sequence in H6 that no other side chains, besides the two conserved thiol groups, are likely to participate in metal coordination during transport. The Pro in CPC, located in the center of the membrane, is characteristic of all P-type ATPases (Axelsen & Palmgren, 1998). The crystal structure of the SR Ca-ATPase shows that probably because of this Pro, helix H4 is unwound in this protein (Toyoshima et al., 2000). If this were the case in P_{1B}-ATPases, it would likely allow the participa-

Table 1. Subgroup IB-1 of P_{1B}-type ATPases

AC #[1]	Genus species	Gene name	MBD[2]	AC #	Genus species	Gene name	MBD
AAK99445	*Streptococcus pneumoniae*	CTPA	0	Q8TR42	*Methanosarcina acetivorans*	MA1342	3
AAM99291	*Streptococcus agalactiae*	*SAG0385*	1	*Q8UF71*	*Agrobacterium tumefaciens*	*ATU1528*	1
AAN24246	*Bifidobacterium longum*	*SILP*	0	Q8UG47	*Agrobacterium tumefaciens*	*ATU1195*	2
AAN47793	*Leptospira interrogates*	*ATC*	1	Q8UGU8	*Agrobacterium tumefaciens*	*ATU0937*	1
AAN54744	*Shewanella oneidensis*	SO1689	1	Q8XMY3	*Clostridium perfringens*	CPE0555	3
AAN55393	*Shewanella oneidensis*	SO2359	3	Q8XU45	*Ralstonia solanacearum*	RSC3348	1
AAN62846	*Colletotrichum lindemuthianum*	CLAP1	3	Q8XZX1	*Ralstonia solanacearum*	RSC1274	2
AAN66213	*Pseudomonas putida*	PP0586	2	Q8Y647	*Listeria monocytogenes*	LMO1853	1
AAN69841	*Pseudomonas putida*	PP4261	3	Q8YEZ7	*Brucella melitensis*	BMEI1730	2
AAO05761	*Staphylococcus epidermidis*	SE2119	2	Q8YFF3	*Brucella melitensis*	BMEI1569	1
AAO08776	*Vibrio vulnificus*	VV10239	3	Q8YQN8	*Anabaena* sp.	ALL3782	1
AAO10964	*Vibrio vulnificus*	VV12614	3	Q8YWI6	*Anabaena* sp.	ALR1627	1
BAC09472	*Thermosynechococcus elongates*	TLL1920	1	Q8ZCA7	*Yersinia pestis*	YPO3086	3
BAC13098	*Oceanobacillus iheyensis*	OB1142	2	Q8ZR95	*Salmonella typhimurium*	STM0498	2
BAC17217	*Corynebacterium efficiens*		1	Q8ZRG7	*Salmonella typhimurium*	STM0353	1
BAC44663	*Mycoplasma penetrans*	MYPE8710	0	Q8ZS77	*Anabaena* sp.	ALR7635	1
BAC45965	*Bradyrhizobium japonicun*	bll0700	0	Q8ZSB9	*Anabaena* sp.	ALL7592	0
EEA00442	*Anopheles gambiae*		3	Q8ZUJO	*Pyrobaculum aerophilum*	PAE2758	1
NP.657694	*Bacillus anthracis A2012*		2	Q92AF5	*Listeria innocua*	LIN1967	1
O17737	*Caenorhabditis elegans*	CUA-1	3	Q92ZA2	*Rhizobium meliloti*	RA0589	1
O26033	*Helicobacter pylori*	HP1503	3	Q92ZX3	*Rhizobium meliloti*	RA0325	1
O27578	*Methanobacterium thermoautotrophicum*	MTH1535	2	Q939V8	*Acinetobacter* sp. *BW3*	CESC	0
O29777	*Archaeoglobus fulgidus**	AF0473	1	Q93HTO	*Bradyrhizobium elkanii*	FIXI	1
O30733	*Rhodobacter capsulatus*	CCOI	1	Q941L1	*Brassica napus*		2
O32220	*Bacillus subtilis*	YvgX	2	Q96WX3	*Candida albicans*	CCC2	2
O32619	*Helicobacter felis*	COPA	1	Q96ZX6	*Sulfolobus tokodaii*	ST1715	1
O33533	*Rhizobium leguminosarum*	FIXI	1	Q978Z8	*Thermoplasma volcanium*	TV1264	0
O59666	*Schizosaccharomyces pombe*	SPBC29A3	1	Q97D27	*Clostridium acetobutylicum*	CAC3655	2
O67432	*Aquifex aeolicus*	AQ1445	1	Q97RR4	*Streptococcus pneumoniae*	SP0729	0
O83999	*Treponema pallidum*	TP1036	1	Q97VH4	*Sulfolobus solfataricus*	SS02651	1
P18398	*Rhizobium meliloti*	RA0659	1	Q988R8	*Rhizobium loti*	MLL6624	1
P32113	*Enterococcus hirae**	COPA	1	Q989H6	*Rhizobium loti*	MLR6417	1
P35670	*Homo sapiens**	ATP7B/WND	6	Q98C24	*Rhizobium loti*	MLR5325	1
P37279	*Synechococcus PCC7942**	PACS	1	Q99R80	*Staphylococcus aureus*	SAV2557	2
P37385	*Synechococcus PCC7942**	SYNA	1	Q9A8E7	*Caulobacter crescentus*	CC1407	1
P38360	*Saccharomyces cerevisiae*	PCA1	1	Q9C594	*Arabidopsis thaliana*	HMA6	1
P38995	*Saccharomyces cerevisiae**	CCC2	2	Q9CHA4	*Lactococcus lactis*	LL0834	1
P46839	*Mycobacterium leprae*	ML1987	1	Q9CJU9	*Pasteurella multocida*	PM1892	1
P46840	*Mycobacterium leprae*	ML2000	1	Q9F3R6	*Ralstonia metallidurans*	COPF	1
P49015	*Cricetulus griseus*	ATP7A	6	Q9F682	*Streptococcus mutans*		1
P55989	*Helicobacter pylori*	HP1072	1	Q9HJ30	*Thermoplasma acidophilum*	Tal143	0
P58341	*Rhizobium meliloti*	ACTP1	2	Q9HN90	*Halobacterium* sp.	VNG2201 G	3
P58342	*Rhizobium meliloti*	ACTP2	2	Q9HRH2	*Halobacterium* sp.	VNG0700 G	2
P70705	*Rattus norvegicus*	ATP7A	6	Q9HX93	*Pseudomonas aeruginosa*	PA3920	2
P72343	*Rhodobacter sphaeroides*	RDXI	2	Q9I3G8	*Pseudomonas aeruginosa*	PA1549	3
P73241	*Synechocystis PCC6803*	SLL1920	1	Q9JU22	*Neisseria meningitidis-Z2491*	NMA1539	3
P74512	*Synechocystis PCC6803*	SLR1950	1	Q9JU88	*Neisseria meningitidis-Z2491*	NMA1444	1
P77868	*Haemophilus influenzae*	HI290	1	Q9K3L4	*Neisseria meningitidis-MD58*	NMB1325	1
P77881	*Listeria monocytogenes*	CTPA	0	Q9KFC7	*Bacillus halodurans*	BH0557	2
P77894	*Mycobacterium tuberculosis*	CTPV	0	Q9KPZ7	*Vibrio cholerae*	VC2215	3
P96875	*Mycobacterium tuberculosis*	CTPC	0	Q9KS24	*Vibrio cholerae*	VC1437	3
Q04656	*Homo sapiens**	ATP7A/MNK	6	Q9KW64	*Pseudomonas syringae*		2
Q10876	*Mycobacterium tuberculosis*	RV0092	1	Q9PND4	*Campylobacter jejuni*	Cj1161c	1
Q10877	*Mycobacterium tuberculosis*	RV0103C	1	Q9PNE0	*Campylobacter jejuni*	Cj1155c	3
Q59207	*Bradyrhizobium japonicum*	FixI	1	Q9PQUO	*Ureaplasma urealyticum*	UU203	0
Q59385	*Escherichia coli*	YbaR	2	Q9QUG4	*Rattus norvegicus*	ATP7B	5
Q59688	*Proteus mirabilis*		2	Q9RDJ4	*Streptomyces coelicolor*	SCO2731	1
Q64430	*Mus musculus**	ATP7A	6	Q9RRN5	*Deinococcus radiodurans*	DR2453	2

Continued on next page

Table 1. Continued

AC #[1]	Genus species	Gene name	MBD[2]	AC #	Genus species	Gene name	MBD
Q64446	*Mus musculus**	ATP7B	5	Q9S7J8	*Arabidopsis thaliana**	RAN1	2
Q8KE75	*Chlorobium tepidum*	CT0815	1	Q9SH30	*Arabidopsis thaliana*	HMA5	2
Q8KJP5	*Rhizobium loti*	FIXI	1	Q9SZC9	*Arabidopsis thaliana*	PAA1	1
Q8KLH2	*Rhizobium etli*	FIXI	1	Q9UVL6	*Candida albicans*	CRP1	5
Q8KWW2	*Pseudomonas putida*	CUEA	2	Q9VYT4	*Drosophila melanogaster*	CG1886	4
Q8NTC1	*Corynebacterium glutamicum*	CGL0386	1	Q9WYF3	*Thermotoga maritime*	TM0317	1
Q8NZV1	*Streptococcus pyogenes*	SPYM18–724	1	Q9X5V3	*Rhizobium leguminosarum*	ACTP	1
Q8PUK6	*Methanosarcina mazei*	MM2328	3	Q9X5X3	*Rhizobium meliloti*	ACTP	2
Q8R7F1	*Thermoanaerobacter tengcongensis*	TTE2463	2	Q9XT50	*Ovis aries*	ATP7B	6
Q8RGP1	*Fusobacterium nucleatum*	FN0245	1	Q9YBZ6	*Aeropyrum pernix*	APE1454	1
Q8RNP6	*Legionella pneumophila*	COPA1	1	Q9ZHC7	*Salmonella typhimurium*	SILP	1
Q8TH11	*Pyrococcus furiosus*	PF0740	2	ZP_00000301	*Ferroplasma acidarmanus*		0

[1] Accession number
[2] Indicates the number of N-MBDs (CXXC) present in each protein.
* Indicates that function has been established by measuring metal transport, metal-dependent ATPases or functional complementation.

Table 2. Subgroup IB-2 of P_{1B}-type ATPases

AC #[1]	Genus species	Gene name	MBD[2]	AC #	Genus species	Gene name	MBD
AAN00131	*Streptococcus agalactiae*	SAG1257	1	Q8XSZ8	*Ralstonia solanacearum*	RSP0319	1▼♦
AAN62190	*Pseudomonas aeruginosa*		▼	Q8YJM9	*Brucella melitensis*	BMEI0053	2♦
AAN70704	*Pseudomonas putida*	cadA-2	▼♦	Q8Z255	*Salmonella typhi*	STY4235	1
AAO03672	*Staphylococcus epidermidis*	SE0075	2	Q8ZAI1	*Yersinia pestis*	YPO3820	2♦
AAO10452	*Vibrio vulnificus*	VV12063	1	Q8ZS90	*Anabaena* sp.	ALR7622	1♦
BAC12232	*Oceanobacillus iheyensis*	OB0276	1	Q926K0	*Listeria innocua*	PLI0061	1
O26511	*Methanobacterium thermoautotrophicum*	MTH411	1	Q92T56	*Rhizobium meliloti*	R00124	1♦
O32219	*Bacillus subtilis**	YVGW	1	Q93GJ9	*Bacillus stearothermophilus*	CADA	1
O33448	*Proteus mirabilis*	PPAA	1	Q93TP6	*Pseudomonas putida*	CADA	▼
O64474	*Arabidopsis thaliana*	HMA4	▼	Q97GX4	*Clostridium acetobutylicum*	CAC2241	1
P20021	*Staphylococcus aureus* (*pI258*)	CADA	1	Q98IB8	*Rhizobium loti*	MLL2475	1♦
P30336	*Bacillus firmus*	CADA	1	Q9AKR5	*Ralstonia metallidurans*	PBRA	▼
P37386	*Staphylococcus aureus*	CADA	2	Q9HSN5	*Halobacterium* sp.	VNG0149G	1
P37617	*Escherichia coli**	ZNTA	1	Q9HXV0	*Pseudomonas aeruginosa*	PA3690	▼♦
P58414	*Listeria monocytogenes*	LMO1100	1	Q9JRM2	*Xanthomonas maltophilia*	CADA	1
P94888	*Lactococcus lactis*	CADA	1	Q9K5Q2	*Bacillus halodurans*	BH4036	1
Q59465	*Helicobacter pylori**	HP0791	1♦	Q9KT72	*Vibrio cholerae*	VC1033	1
Q59998	*Synechocystis PCC6803**	ZIAA	1♦	Q9RQB4	*Helicobacter felis*		1
Q60048	*Listeria monocytogenes**	CADA	1	Q9RZ81	*Deinococcus radiodurans*	DRA0073	1
Q8L158	*Oscillatoria brevis*	BXA1	▼♦	Q9SZW4	*Arabidopsis thaliana*	HMA2	▼
Q8R7E7	*Thermoanaerobacter tengcongensis*	ZNTA2	1	Q9SZW5	*Arabidopsis thaliana*	HMA3	▼
Q8RGN3	*Fusobacterium nucleatum*	FN0258		Q9V060	*Pyrococcus abyssi*	PAB0626	1♦
Q8RNN4	*Legionella pneumophila*	CADA2	▼	Q9ZL53	*Helicobacter pylori*	HmcT	1♦
Q8UH42	*Agrobacterium tumefaciens*	ATU0843	2♦				

[1] Accession number.
[2] Indicates the number of CXXC N-MBDs present in each protein.
▼ Indicates that a Cys in the consensus MBD is mutated.
♦ Indicates one or more putative $(HX)_n$ MBD.
* Indicates that function has been established by measuring metal transport, metal-dependent ATPase activity or functional complementation.

tion of both Cys side chains in metal coordination. Eight positions downstream of the central Pro in H6, an additional Pro is present in all but three of the available P_{1B}-ATPase sequences. It is interesting that the location of this second Pro corresponds with the proposed cytoplasmic entrance into the transmembrane ion path of the SR Ca-ATPase (Toyoshima & Nomura, 2002).

Analysis of the sequences of H7-H8 shows that those residues with side chain atoms able to coordinate metals are highly conserved (Fig. 2*B*). In a pattern that is somewhat repeated in H8, there is a

Table 3. Subgroup IB-3 of P_{1B}-type ATPases

AC #[1]	Genus species	Gene name	MBD	AC #	Genus species	Gene name	MBD
AAN00136	*Streptococcus agalactiae*	SAG1262	♦	Q59369	*Escherichia coli*	HRA-1	♦
AAO03723	*Staphylococcus epidermisdis*	SE0126	♦	Q59370	*Escherichia coli*	HRA-2	♦
BAC13677	*Oceanobacillus iheyensis*	OB1721	♦	Q8NL10	*Corynebacterium glutamicum*	CGL2962	♦
BAC17091	*Corynebacterium efficiens*			Q8PWW3	*Methanosarcina mazei*	MM1463	♦
O26849	*Methanobacterium thermoautotrophicum*	MTH755	♦	Q8TUA7	*Methanosarcina acetivorans*	MA0166	♦
O30085	*Archaeoglobus fulgidus**	AF0152	♦	Q8VPE6	*Enterococcus faecium*	TCRB	♦
O67203	*Aquifex aeolicus*	AQ1125	♦	Q9CH87	*Lactococcus lactis*	LL0851	♦
P05425	*Enterococcus hirae**	COPB	♦	Q9JP67	*Lactobacillus sakei*	ATKB	♦

[1] Accession number.
* Indicates that function has been established by measuring metal transport or metal-dependent ATPase activity.
♦ Indicates a His-rich MBD.

Table 4. Subgroup IB-4 of P_{1B}-type ATPases

AC #[1]	Genus species	Gene name	MBD	AC #	Genus species	Gene name	MBD
AAN59655	*Streptococcus mutans*	SMU.2057c		Q8YDS8	*Brucella melitensis*	BMEII0097	
AAN65675	*Pseudomonas putida*	cadA-1		Q8YSC8	*Anabaena sp.*	ALL3161	
AAO03659	*Staphylococcus epidermidis*	SE0062	♦	Q92E17	*Listeria innocua*	LIN0644	
BAC19804	*Corynebacterium efficiens*			Q99Z27	*Streptococcus pyogenes*	SPY1434	
NP_464168	*Listeria monocytogenes*			Q9A4U9	*Caulobacter crescentus*	CC2726	
O31688	*Bacillus subtilis*	YKVW		Q9K1U0	*Chlamydia pneumoniae*	CP1001	
O53160	*Mycobacterium tuberculosis*	RV1469		Q9KEV5	*Bacillus halodurans*	BH0744	
O68082	*Rhodobacter capsulatus*			Q9M3H5	*Arabidopsis thaliana*	HMA1	♦
O69710	*Mycobacterium tuberculosis*	RV3743c		Q9PLJ9	*Chlamydia muridarum*	TC0100	
O84732	*Chlamydia trachomatis*	CT727		Q9ZBF3	*Streptomyces coelicolor*	SC9B5.27	
Q59997	*Synechocystis PCC6803**	SLR0797/COAT					

[1] Accession number.
* Indicates that function has been established by functional complementation.
♦ Indicates a His-rich MBD.

Table 5. Subgroups IB-5 and IB-6 of P_{1B}-type ATPases

Subgroup IB-5			Subgroup IB-6			
ExPASy #	Genus species	Gene name	AC #[1]	Genus species	Gene name	H6
BAC18750	*Corynebacterium efficiens*		Q10866	*Mycobacterium tuberculosis*	RV1992C	APC
Q8NT32	*Corynebacterium glutamicum*	CGL0482	Q8RNN5	*Legionella pneumophila*	CADA1	APC
Q92Z60	*Rhizobium meliloti*	RA0632	Q9I147	*Pseudomonas aeruginosa*	PA2435	CPC
Q988U4	*Rhizobium loti*	MLL6590	Q9Y8R2	*Aeropyrum pernix*	APE2571	CPS
Q9RJ01	*Streptomyces coelicolor*	SCJ1.13	S60899	*Helicobacter pylori*		CPS

[1] Accession number.
H6 Indicates the putative metal binding sequence present in H6.

conserved Asn in the cytoplasmic end and a Pro in the luminal or extracellular end of H7. It is interesting that similar to the Pro at the end of H6, an Asn is present at the cytoplasmic end of H7 in all P_{1B}-ATPases (except in subgroup IB-5), while an Asn/Ser is present at the cytoplasmic end of H8. In the center of H7 a Tyr-Asn is completely conserved. As a counterpart, H8 has a conserved $Met(Xxx)_2SerSer$ sequence. Because of their relatively high hydrophilicity, these residues likely face the interior of the protein, i.e., the metal path. Furthermore, these particular residues appear to be true signature sequences since a search of SWISS-PROT, TrEMBL, and TrEMBL-New databases with the ScanProsite using the consensus NX(6)YNX(4)PX(5,25)PX(6)MXXSSX(5)[NS] re-

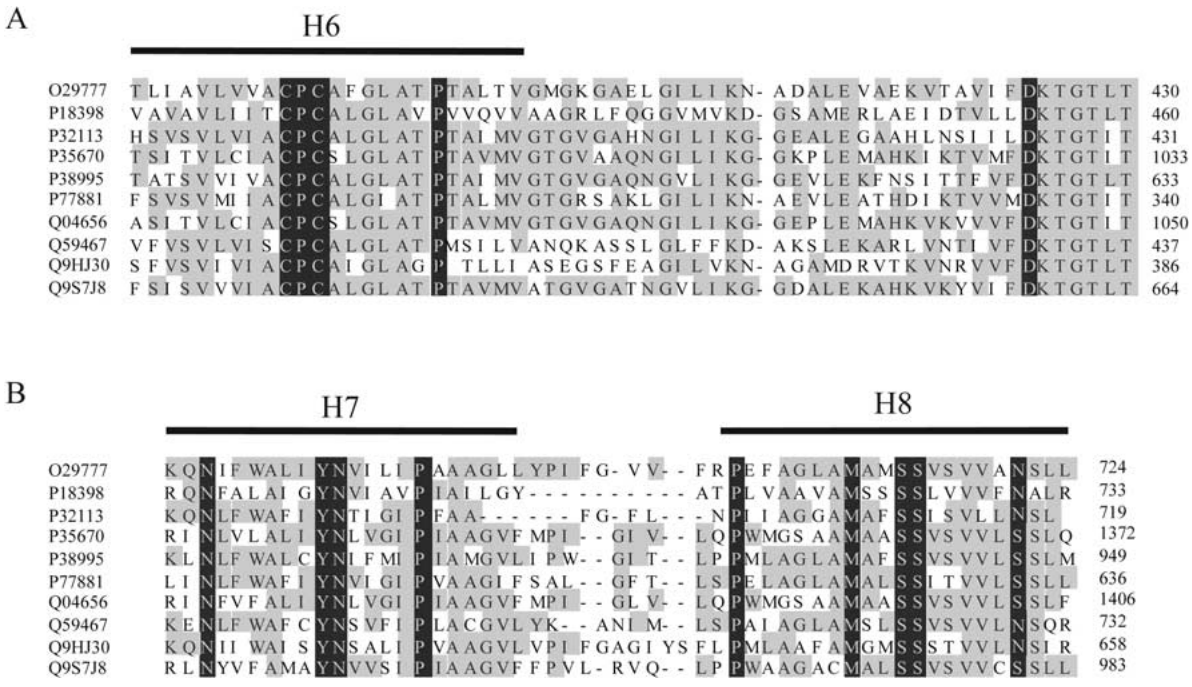

Fig. 2. Alignments of the H6 (*A*) and H7-H8 (*B*) regions of ten representative members of subgroup IB-1. Proteins are listed under their accession numbers (*left column*). The positions of the last residue in the aligned fragments are listed in the *right column*. The Asp in the DKTGT consensus conserved in all P-type ATPases is highlighted by dark grey. Residues conserved in all members of this subgroup and that have potential metal-coordinating side chains are also highlighted by dark grey background. Light grey background indicates that the residue is conserved in most members of this subgroup.

turned only members of this subgroup (similar analysis using randomized databases did not return any sequence). Supporting the tested hypothesis, analysis of other TMs of these proteins (H1–5) did not reveal conserved residues containing potential metal coordinating side chains. Thus, the analysis suggests that the coordination of Cu^+ and Ag^+, when transported by P_{IB-1} ATPases, is achieved by the conserved amino acids in TMs H6 (2 Cys), H7 (Tyr and Asn) and H8 (Met and 2 Ser).

A singular characteristic of P_{1B}-ATPases is that many of them have additional metal-binding domains located in their N-terminal cytoplasmic end (N-MBD). Although it is apparent that there are different types of N-MBDs (*see* below), the most frequent ones are characterized by a CXXC sequence. Identified in early studies of the Menkes and Wilson diseases proteins (Bull & Cox, 1994; Vulpe & Packman, 1995), these approximately 60-amino-acid-long domains appear in five/six repeats in mammalian proteins. However, most proteins in Subgroup IB-1 have only two, one, or even lack an N-MBD (Table 1). The absence of N-MBDs in many of the IB-1 proteins supports studies proposing a regulatory rather than an essential role for these domains in the catalytic mechanism of P_{1B}-ATPases (Mitra & Sharma, 2001; Tsivkovskii, MacArthurs & Lutsenko, 2001; Voskoboinik et al., 2001; Fan & Rosen, 2002). The N-MBDs present in subgroup IB-1 are homologous to a number of metal chaperone proteins (Arnesano et al., 2002), can bind Cu^+, Cu^{2+}, Zn^{2+}, Cd^{2+} (DiDonato et al., 1997), and exchange metals with the related chaperones through a simple equilibrium ($K_{eq} \approx 1$) (Huffman & O'Halloran, 2000). The NMR structure of the fourth N-MBD of the Menkes protein clearly points out the similarities between these domains and metal chaperones (Gitschier et al., 1998). The presence of at least one intact N-MBD is required for targeting of Menkes and Wilson proteins from the trans-Golgi network to the plasma membrane and a vesicular compartment, respectively (Camakaris et al., 1995; Petris et al., 1996; Schaefer et al., 1999). Mutation of both Cys does not produce significant changes in the affinity of these enzymes for their substrates (metal and ATP-Mg) but leads to an important decrease in V_{max} (Voskoboinik et al., 2001; Fan & Rosen, 2002). We have observed that this diminished V_{max} is due to a reduction in the enzyme-dephosphorylation rate (Mandal and Argüello, unpublished results). Interestingly, Lutsenko and coworkers showed that the Wilson's N-MBDs interact with the enzyme large cytoplasmic loop in a Cu^+-dependent manner (Tsivkovskii et al., 2001). This loop, responsible for ATP binding and hydrolysis, is where the catalytic phosphorylation of the enzyme occurs (Fig. 1).

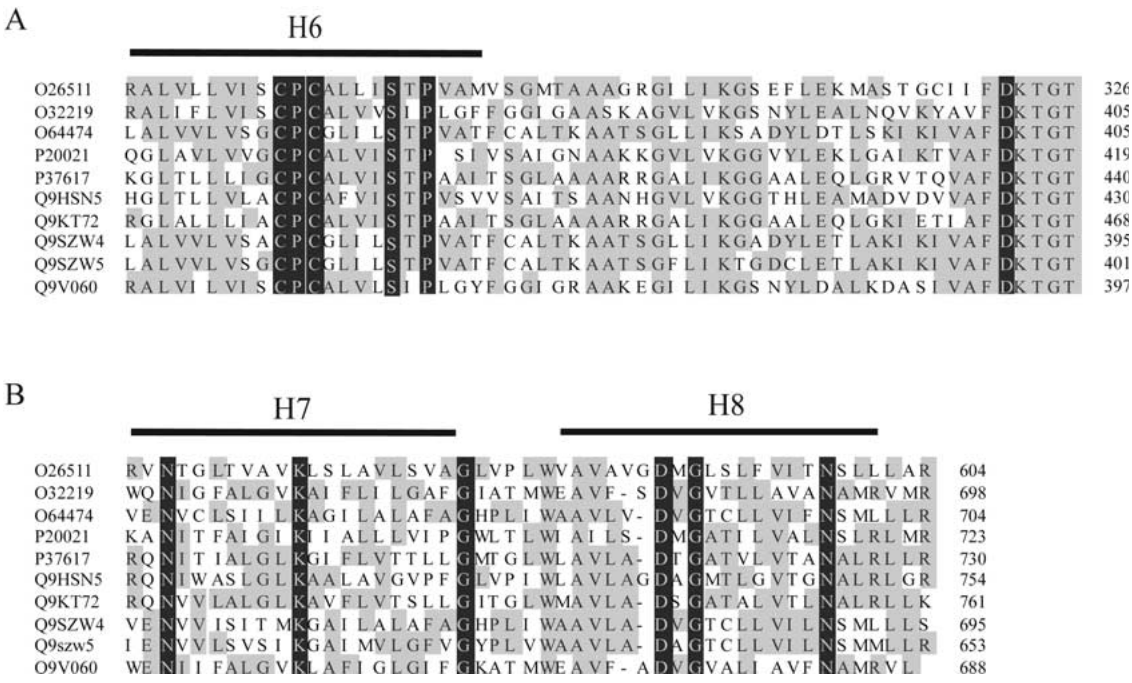

Fig. 3. Alignments of the H6 (*A*) and H7-H8 (*B*) regions of ten representative members of subgroup IB-2. Proteins are listed under their accession numbers (*left column*). The positions of the last residue in the aligned fragments are listed in the *right column*. The Asp in the DKTGT consensus conserved in all P-type ATPases is highlighted by dark grey. Residues conserved in all members of this subgroup and that have potential metal- coordinating side chains are also highlighted by dark grey background. Light grey background indicates that the residue is conserved in most members of this subgroup.

Structural-Functional Characteristics of Subgroup IB-2

Group *IB*-2 comprises 47 sequences (Table 2). Among the proteins included in this group, *E. coli* ZntA (P37617) (Okkeri & Haltia, 1999; Sharma et al., 2000), *H. pylori* CadA (Q54463) (Herrmann et al., 1999), *S. aureus* (p1258) CadA (P20021) (Tsai & Linet, 1993; Rensing et al., 1998), *Synechocystis* PCC6803 ZiaA (Q59998) (Thelwell, Robinson & Turner-Cavet, 1998), *L. monocytogenes* CadA (Q60048) (Bal et al., 2001), and *B. subtilis* CadA (O32219) (Tsai et al., 1992) have been characterized as $Zn^{2+}/Cd^{2+}/Pb^{2+}$-ATPases. Interestingly, these Zn-ATPases have been found in archaea, prokaryotes and plants, but not in other eukaryotes. The *Arabidopsis* genome contains three proteins of this subgroup (HMA2 (Q9SZW4), HMA3 (Q9SZW5) and HMA4 (O64474)) and ESTs encoding similar proteins have been identified in other plant genomes being sequenced (*see* cotton, tomato, etc. in www.tigr.org). Figure 3 shows the alignment of H6 and H7-H8 of ten representative members of group IB-2. H6 has the $CPC(X)_4[S/T]XP$ sequence similar to that present in subgroup IB-1. However, in this case a Ser or Thr hydroxyl is present in the sixth position downstream the central Pro and perhaps contributes to metal transport. Contrasting with H6, conserved residues in H7-H8 are clearly distinct in subgroup IB-2. Two Asn are conserved in the cytoplasmic sides of both TMs, while a Lys in H7 and AspXxxGly in H8 appear fully conserved. These key residues located in the center of the membrane provided the signature sequence NX(7)KX(10,20)DXGX(7)N that returns only IB-2 subgroup ATPases. The presence of a fully conserved Lys in H7 is particularly interesting. This might perhaps interact via salt bridge with the Asp in H8; however, most likely it is part of a second shell interaction that stabilizes the bound Zn (Dudev et al., 2003). In any case, the conserved residues suggest a particular metal coordination likely to include amino and carboxyl groups, thus a unique selectivity distinct from that of subgroup IB-1, although both groups share the same CPC sequence.

The N-terminal fragment of proteins in the IB-2 subgroup extends between 100 and 150 amino acids. Most of these enzymes possess one (and exceptionally two) N-MBD containing the CXXC sequence (Table 2). The functional role of the CXXC N-MBD in *E. coli* ZntA (P37617) has been studied (Mitra & Sharma, 2001). This, like the N-MBD of IB-1 ATPases, seems to have a regulatory role. However, a significant number of IB-2 proteins that contain fragments highly homologous to the CXXC N-MBDs (11 among 47) appear to have one of the Cys mutated and the metal-binding capacity probably lost (Table 2). Thirteen proteins in the IB-2 subgroup are also different because of the presence of a different

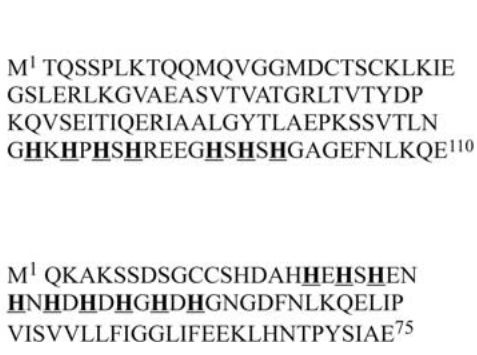

Fig. 4. Examples of His-rich N-MBD present in IB-2-subgroup proteins. The entire N-terminal sequences up to the putative cytoplasmic end of H1 are provided for (*A*) ZiaA from *Synechocystis PCC6803* (Q59998), and (*B*) Bxa1 from *Oscillatoria brevis* (Q8L158). The position of the last residue in each fragment is indicated. His residues within $(HX)_n$ repeats are highlighted.

putative metal-binding domain characterized by $(HX)_n$ repeats ($n = 2$–3) (Fig. 4). Similar MBDs are present in two other types of metal ion transport proteins, the ZIP and the cation diffusion facilitator (CDF) families (Paulsen & Saier, 1997; Eng et al., 1998). However, in these families the $(HX)_n$ repeats are found in loops joining TMs, not at the N-terminus. The functional role of these likely metal-binding domains in the ZIP and CDF family has not been determined. Interestingly, ten of the IB-2 proteins contain both types of putative N-MBD (CXXC and $(HX)_n$). Although both could interact with divalent metals, the functional purpose of the simultaneous presence of different types of MBDs is not self-evident.

Structural-Functional Characteristics of Subgroup IB-3

Group IB-3 includes 16 sequences containing the CPH in H6, unique sequences in H7 and H8, and a distinct His-rich N-MBD (Table 3). There are no eukaryotic proteins in this subgroup. *E. hirae* CopB (PO5425) was the first IB-3 enzyme to be characterized (Odermatt et al., 1993; Solioz & Odermatt, 1995). These studies proposed that the enzyme transports Cu^+/Ag^+. However, recent studies of the homologous *A. fulgidus* CopB (O30085) point out that Cu^{2+} produces a five times larger activation of this enzyme compared to that driven by Cu^+ (and 2.5 times that of Ag^+) (Argüello et al., 2003). Keeping in mind that imidazolium (a hard Lewis base) prefers to bind Cu^{2+} (an "intermediate" Lewis acid) rather than Cu^+ (a soft Lewis base) (Pearson, 1963; Hughes, 1988; Fraústro da Silva & Williams, 2001), the activation of *A. fulgidus* CopB (O30085) by Cu^{2+} is in line with the CPH sequence in H6 and the presence of a His-rich N-MBD.

The region between CPH and the Pro close to the cytoplasmic end of H6 (ALGLA[I/V]) is also highly conserved (Fig. 5). Interestingly, H7 and H8 closely resemble their counterparts in subgroup IB-1. Thus, H7 has the $N(X)_5GYN(X)_4P$ consensus, where the fully conserved Gly before the TyrAsn pair is the only apparent significant change. In a similar fashion H8 resembles that in subgroup IB-1 with a conserved $P(X)MSXST(X)_5N$ sequence (compare to $P(X)_6MXXSS(X)_5N$). In spite of this, the sequence NX(5)GYNX(4)PX(10,20)PX(6)MSXSTX(5)N constitutes a true signature for the IB-3 group. Considering these similarities with proteins from group IB-1, it is not surprising that Cu^+/Ag^+ partially activate these enzymes. On the other hand, the presence of an additional conserved Ser in H8 of the IB-3 subgroup proteins might facilitate the tetragonal coordination geometry favored by Cu^{2+}, alternative to the tetrahedral preferred by Cu^+ (Fraústro da Silva & Williams, 2001).

As mentioned, these proteins contain particular His-rich N-MBDs. Although difficult to evaluate from their primary structure, these appear different from the N-MBD observed in IB-2 proteins ($(HX)_n$ repeats). They have many more His; for instance, *A. fulgidus* CopB (O30085) has 17 His in the 51-amino-acid stretch before H1. In spite of the obvious structural differences, these His-rich N-MBDs appear to have a role similar to that of the CXXC N-MBDs. Truncated *A. fulgidus* CopB (O30085), where the N-MBD was entirely removed, showed no change in metal selectivity or affinities but a 40% decrease in turnover rate (Argüello et al., 2003).

Structural functional characteristics of subgroup IB-4

The 21 sequences in this group are among the smallest P-type ATPases with average length of 620-680 amino acids (Table 4). As in the case of IB-2 subgroup Zn-ATPases, plants are the only eukaryotes with members in the IB-4 subgroup. Most interesting, topological analysis of these sequences with transmembrane prediction software suggests the presence of only six/seven TMs with only five/four in the N-half of the molecule and two downstream of the large cytoplasmic loop that characterizes P-type ATPases (*see* Fig. 8 below). In addition, they lack an N-MBD (except for *S. epidermidis* (AAO03659) and *Arabidopsis* HMA1 (Q9M3H5)) and end shortly after their last putative TM. Thus, it is apparent that these are the simplest P-type ATPases and they might provide a parsimonious model for structural and mechanistic studies on ion transport and energy transduction. A single enzyme of this group has been partially characterized, *Synechocystis* PCC6803 CoaT (Q59997). This protein seems to be involved in Co^{2+} transport

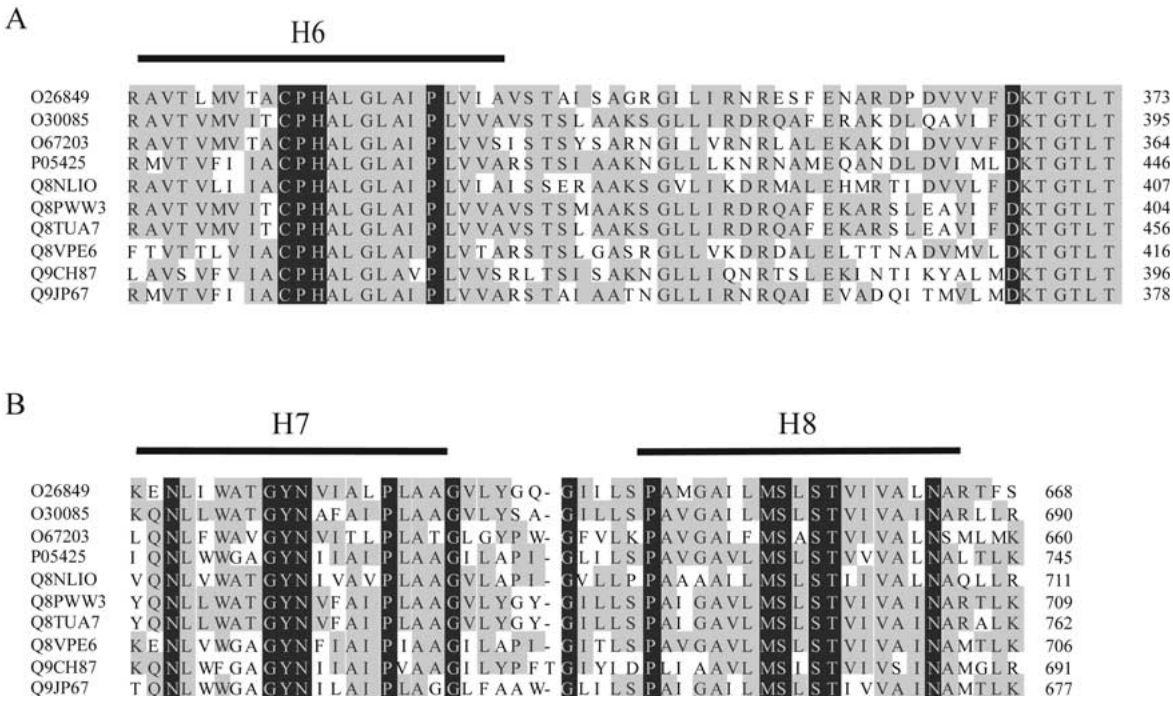

Fig. 5. Alignments of the H6 (*A*) and H7-H8 (*B*) regions of ten representative members of subgroup IB-3. Proteins are listed under their accession numbers (*left column*). The positions of the last residue in the aligned fragments are listed in the *right column*. The Asp in the DKTGT consensus conserved in all P-type ATPases is highlighted by dark grey. Residues conserved in all members of this subgroup and that have potential metal-coordinating side chains are also highlighted by dark grey background. Light grey background indicates that the residue is conserved in most members of this subgroup.

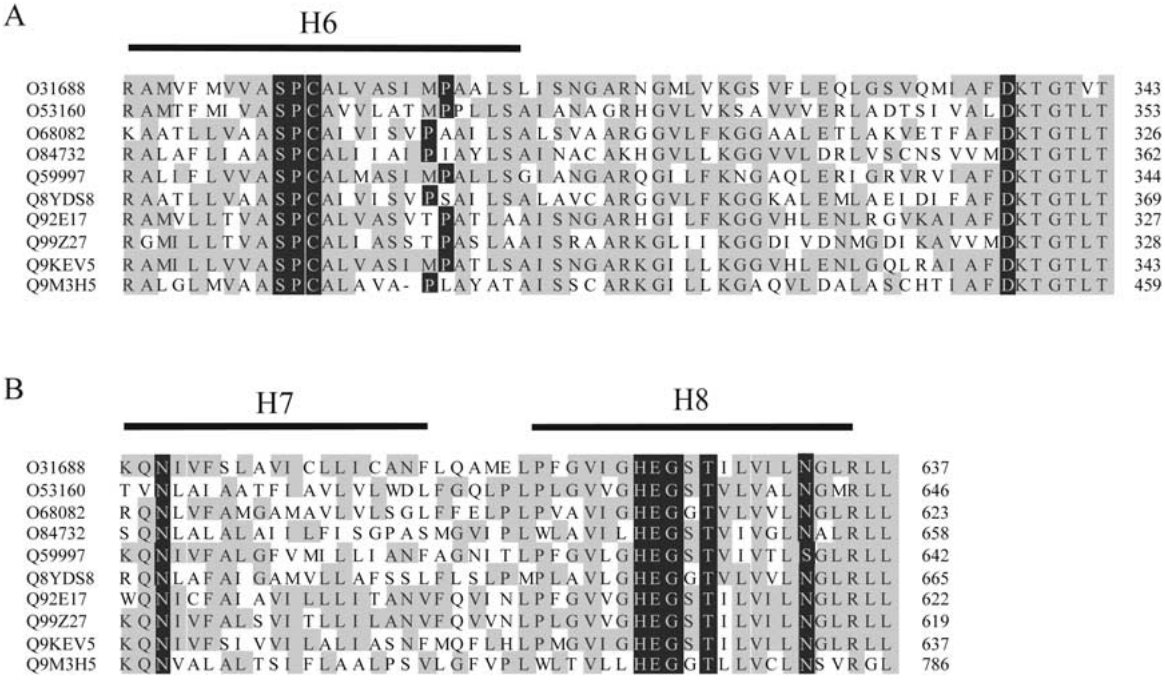

Fig. 6. Alignments of the H6 (*A*) and H7-H8 (*B*) regions of ten representative members of subgroup IB-4. Note that, even though these proteins are likely to have only six or seven TMs, for simplicity we refer to the TM upstream of the phosphorylation site as H6 and to the last two TMs in these proteins as H7 and H8. Proteins are listed under their accession numbers (*left column*). The positions of the last residue in the aligned fragments are listed in the *right column*. The Asp in the DKTGT consensus conserved in all P-type ATPases is highlighted by dark grey. Residues conserved in all members of this subgroup and that have potential metal coordinating side chains are also highlighted by dark grey background. Light grey background indicates that the residue is conserved in most members of this subgroup.

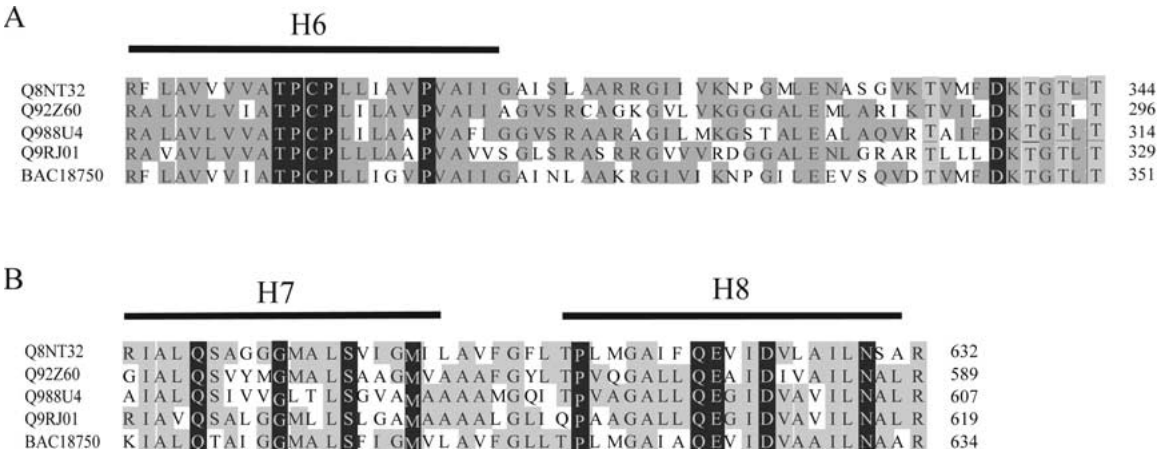

Fig. 7. Alignments of the H6 (*A*) and H7-H8 (*B*) regions of the five members of subgroup IB-5. Note that, even though these proteins are likely to have only six or seven TMs, for simplicity we refer to the TM upstream of the phosphorylation site as H6 and to the last two TMs in these proteins as H7 and H8. Proteins are listed under their accession numbers (*left column*). The positions of the last residue in the aligned fragments are listed in the *right column*. The Asp in the DKTGT consensus conserved in all P-type ATPases is highlighted by dark grey. Residues conserved in all members of this subgroup and that have potential metal-coordinating side chains are also highlighted by dark grey background. Light grey background indicates that the residue is conserved in most members of this subgroup.

since disruption of coaT gene reduced *Synechocystis* Co^{2+} tolerance and increased cytoplasmic Co^{2+} accumulation (Rutherford et al., 1999).

As in the other P_{1B}-ATPases, the only metal-coordinating amino acids in H6 are the Ser and Cys flanking the central Pro (Fig. 6). Similarly, a Pro located seven/eight positions from SPC characterizes the cytoplasmic end of H6. Note that, even though these proteins likely have only six or seven TMs, for simplicity we will continue referring to the TM upstream of the phosphorylation site as H6 and to the last two TMs in these proteins as H7 and H8. Considering H7-H8, no conserved residue was identified in H7 (except for an Asn at the cytoplasmic end), while H8 revealed a HEGT[GS]T(X)5[NS][GSA] signature sequence where again the metal-coordinating side chains (His, Glu, and Thr) are fully conserved. Although H7 has no conserved residues, its involvement in metal coordination through backbone carbonyls cannot be disregarded. A search for putative metal-coordinating, conserved residues in other TMs did not suggest their participation in metal binding.

Structural Characteristics of Subgroup IB-5

Only five sequences are included in this subgroup (Table 5). They are highly homologous with 35–48% identity within the group and an average of 23 ± 3% when compared to other P_{1B}-ATPases (percent identities are based in full-sequence alignments). In addition, they present defined characteristics that set them apart. Five residues are fully conserved in the H6 of these enzymes TPCP(X)5P (Fig. 7). The two Pro at the center of this TM will likely play a key role in the possibility that the Thr and Cys side chains participate in metal coordination. In H7 and H8, several oxygen-containing residues (Gln, Glu, Ser, Asp) are located in the center of these TMs. The presence of these carboxyl groups suggests a distinct selectivity, still to be determined, for these enzymes.

Subgroup IB-6

Five enzymes were not sorted in any of the described subgroups (Table 5). These appear to be P_{1B}-ATPases based on the presence of typical structural characteristics: a) the cytoplasmic phosphorylation site, DKTGT; b) an APC, CPC, or CPS sequence; and c) significant sequence similarity (30–40%) to other P_{1B}-ATPases (as evident in their phylogenetic location, *see* Fig. 9). However, they present distinct sequences in H7 and H8. This prevented assigning a particular selectivity to these enzymes. Further studies might reveal the selectivity of these enzymes and the residues likely participating in metal coordination.

Discussion

The goal of this work was to identify the determinants of metal selectivity in P_{1B}-ATPases. The data presented support the starting hypothesis that metal specificity of P_{1B}-ATPases is provided by amino acids located in H6 and in the two TMs that follow the large cytoplasmic loop of these enzymes (Fig. 8). Through sequence analysis, a number of conserved amino acids that can probably coordinate the metals transported by these enzymes were identified. In turn,

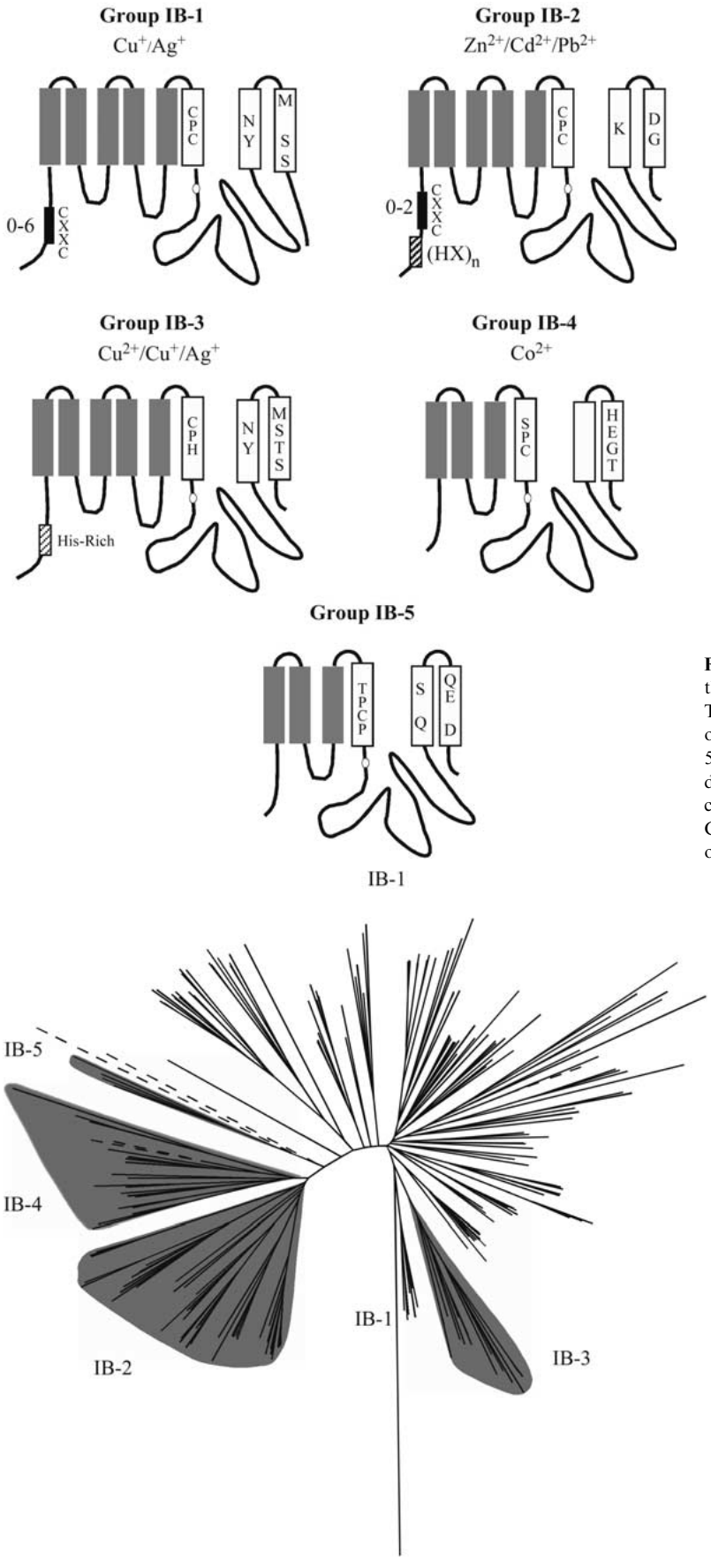

Fig. 8. Summary of the structural characteristics of the five proposed subgroups of P_{1B}-type ATPases. The metal specificity of each subgroup is indicated over each membrane topology, except in group IB-5. Amino acids in TMs proposed to participate in determining metal selectivity are indicated in the corresponding block (*white*). *Black* blocks represent CXXC N-MBDs. *Striped* blocks represent His-rich or $(HX)_n$ N-MBDs.

Fig. 9. Phylogenetic tree of P_{1B}-type ATPases. The tree was prepared from a Clustar W alignment of the whole sequences of the 234 identified in Tables 1, 2, 3, 4 and 5. Branches indicating proteins in subgroups IB-2, IB-3, IB-4 and IB-5 are under shadowed areas. Branches representing proteins in subgroup IB-1 are indicated as continuous lines with no shadow. Dashed lines represent proteins pooled under subgroup IB-6.

these conserved amino acids provide true signature sequences that allow assignment of metal specificity to most P_{1B}-ATPases and predict new metal specificities still to be determined, in particular enzyme subgroups.

In the last decade a number of metal transport-protein families have been identified (ZIP, CDF, ABC-ATPases, P_{1B}-ATPases, etc.) (Brown et al., 1991; Silver & Phung, 1996; Paulsen & Saier, 1997; Eng et al., 1998; Anton et al., 1999; Williams et al., 2000). Subsequent studies have focused on their functional/physiological role, while the relationship between their structural diversity and metal specificity has received modest attention. Thus, there is very little information on transition metal binding sites of membrane transport proteins, although extensive information is available in structural and redox metal sites of proteins. Furthermore, there are no available signature sequences to ensure prediction of metal specificity or that suggest a mechanism of metal coordination during transport. Nevertheless, preliminary assignment of metal specificity is possible for highly homologous proteins when representative examples have been functionally characterized. In the case of P_{1B}-ATPases, phylogenetic analysis has suggested two subgroups of proteins, namely monovalent and divalent metal transporting enzymes (Solioz & Vulpe, 1996; Rensing et al., 1999). This analysis cannot explain the different metal transported by proteins carrying the CPC sequence in H6, nor does it help to predict Co^{2+}-transporting ATPases or other ATPases (carrying CPS or TPC sequences) with metal specificities still to be described.

An alternative approach presented in this report is to analyze those protein regions likely involved in metal transport in search of predicting sequences. In the case of P_{1B}-ATPases, because of their similarities with better-characterized P_{II}-type ATPases, these regions (TMs) can be identified with confidence. As shown, the analysis of these TMs revealed the unique sequences defining the metal specificity of most P_{1B}-ATPases. Five P_{1B}-ATPase subgroups were identified (IB-1/IB-5) with well-defined signature sequences and particular structural characteristics. Figure 8 summarizes these findings. Three of these subgroups, IB-1, IB-2 and IB-3, have well-defined selectivity. An enzyme from group IB-4 has been characterized but further studies might be necessary to confirm the transported metal. It is interesting that the analysis of the TMs of P_{1B}-ATPases also revealed new subgroups with likely different metal specificities. Preliminary experiments underway in our laboratory support this hypothesis.

Subgroups IB-1/5 were identified by analyzing H6, H7 and H8. However, as could be expected, proteins within a subgroup are phylogenetically related. Figure 9 shows the phylogenetic tree resulting from whole-sequence alignment of the 234 P_{1B}-ATPase sequences. This shows that proteins in subgroup IB-2, IB-4 and IB-5 constitute clearly separated branches of this subfamily. In contrast, IB-3 proteins are closely related to those in IB-1 and probably evolved from them. Similarly, those proteins pooled in subgroup IB-6 (dashed lines in Fig. 9) seem to have emerged from one of the main five groups.

Different mechanisms can be postulated to explain ion selectivity by heavy metal transport proteins. Ion charge, size, coordination geometry, or Lewis acid/base strength might all play a role. In the case of P_{1B}-ATPases, the metal specificity appears determined by a variety of putative metal-coordinating side chains (thiol, imidazolium, amide, amine, hydroxyl, carboxyl) and probably backbone carbonyls. Although this requires experimental confirmation, it suggests a key role for the acid/base properties of the metals and residue side chains in the ion discrimination by P_{1B}-ATPases.

I thank Kristin Wobbe and Atin Mandal for helpful discussions and critical review of the manuscript, and Win Cheung and Melinda Palma for their assistance with sequence download, file organization and listing. This work was supported by the National Institute of Health Grant R15 GM64419 and American Chemical Society—The Petroleum Research Fund Grant #36628-AC.

References

Altschul, S.F., Gish, W., Miller, W., Myers, E.W., Lipman, D.J. 1990. Basic local alignment search tool. *J. Mol. Biol.* **215:**403–410

Anton, A., Grosse, C., Reissmann, J., Pribyl, T., Nies, D.H. 1999. CzcD is a heavy metal ion transporter involved in regulation of heavy metal resistance in Ralstonia sp strain CH34. *J. Bacteriol.* **181:**6876–6881

Argüello, J.M., Kaplan, J.H. 1994. Glutamate 779, an intramembrane carboxyl, is essential for monovalent cation binding by the Na,K-ATPase. *J. Biol. Chem.* **269:**6892–6899

Argüello, J.M., Lingrel, J.B. 1995. Substitutions of serine 775 in the alpha subunit of the Na,K-ATPase selectively disrupt K^+ high affinity activation without affecting Na^+ interaction. *J. Biol. Chem.* **270:**22764–22771

Argüello, J.M., Mandal, A.K., Mana-Capelli, S. 2003. Heavy metal transport CPx-ATPases from the thermophile *Archaeoglobus fulgidus*. *In*: Na,K-ATPase and Related Cation Pumps: Structure, Function, and Regulatory Mechanisms. Jørgensen, P.L., Karlish, S.J.D., and Maunsbach, A.B. editors. Annals of New York Academy of Sciences, NY, Vol. 986, pp. 212–218

Argüello, J.M., Peluffo, R.D., Feng, J., Lingrel, J.B., Berlin, J.R. 1996. Substitution of glutamic 779 with alanine in the Na,K-ATPase alpha subunit removes voltage dependence of ion transport. *J. Biol. Chem.* **271:**24610–24616

Argüello, J.M., Whitis, J., Cheung, M.C., Lingrel, J.B. 1999. Functional role of oxygen-containing residues in the fifth transmembrane segment of the Na,K-ATPase alpha subunit. *Arch. Biochem. Biophys.* **364:**254–263

Arnesano, F., Banci, L., Bertini, I., Ciofi-Baffoni, S., Molteni, E., Huffman, D.L., O'Halloran, T.V. 2002. Metallochaperones and metal-transporting ATPases: a comparative analysis of sequences and structures. *Genome Res.* **12:**255–271

Axelsen, K.B., Palmgren, M.G. 1998. Evolution of substrate specificities in the P-type ATPase superfamily. *J. Mol. Evol.* **46:**84–101

Axelsen, K.B., Palmgren, M.G. 2001. Inventory of the superfamily of P-type ion pumps in *Arabidopsis*. *Plant Physiol.* **126:**696–706

Bal, N., Mintz, E., Guillain, F., Catty, P. 2001. A possible regulatory role for the metal-binding domain of CadA, the *Listeria monocytogenes* Cd^{2+}-ATPase. *FEBS Lett.* **506:**249–252

Bissig, K.D., Wunderli-Ye, H., Duda, P.W., Solioz, M. 2001. Structure-function analysis of purified *Enterococcus hirae* CopB copper ATPase: effect of Menkes/Wilson disease mutation homologues. *Biochem. J.* **357:**217–223

Brown, N.L., Camakaris, J., Lee, B.T., Williams, T., Morby, A.P., Parkhill, J., Rouch, D.A. 1991. Bacterial resistances to mercury and copper. *J. Cell. Biochem.* **46:**106–114

Bull, P.C., Cox, D.W. 1994. Wilson disease and Menkes disease: new handles on heavy-metal transport. *Trends Genet.* **10:**246–252

Bull, P.C., Thomas, G.R., Rommens, J.M., Forbes, J.R., Cox, D.W. 1993. The Wilson disease gene is a putative copper transporting P-type ATPase similar to the Menkes gene [published erratum appears in *Nat. Genet.* 1994. **6:**214]. *Nat. Genet.* **5:**327–337

Camakaris, J., Petris, M.J., Bailey, L., Shen, P., Lockhart, P., Glover, T.W., Barcroft, C., Patton, J., Mercer, J.F. 1995. Gene amplification of the Menkes (MNK; ATP7A) P-type ATPase gene of CHO cells is associated with copper resistance and enhanced copper efflux. *Hum. Mol. Genet.* **4:**2117–2123

Cowan, J.A. 1996. Inorganic Biochemistry. An Introduction. Wiley-VCH, Inc., New York, NY

DiDonato, M., Narindrasorasak, S., Forbes, J.R., Cox, D.W., Sarkar, B. 1997. Expression, purification, and metal binding properties of the N-terminal domain from the Wilson disease putative copper-transporting ATPase (ATP7B). *J. Biol Chem.* **272:**33279–33282

Dudev, T., Lin, Y.L., Dudev, M., Lim, C. 2003. First-second shell interactions in metal binding sites in proteins: A PDB survey and DFT/CDM calculations. *J. Am. Chem. Soc.* **125:**3168–3180

Dutzler, R., Campbell, E.B., Cadene, M., Chait, B.T., MacKinnon, R. 2002. X-ray structure of a ClC chloride channel at 3.0 A reveals the molecular basis of anion selectivity. *Nature* **415:**287–294

Eng, B.H., Guerinot, M.L., Eide, D., Saier, M.H., Jr. 1998. Sequence analyses and phylogenetic characterization of the ZIP family of metal ion transport proteins. *J. Membrane Biol.* **166:**1–7

Fan, B., Rosen, B.P. 2002. Biochemical characterization of CopA, the Escherichia coli Cu(I)- translocating P-type ATPase. *J. Biol. Chem.* **277:**46987–46992

Felsenstein, J. 1989. PHYLIP—Phylogeny Inference Package (Version 3.2). *Cladistics* **5:**164–166

Fraústro da Silva, J.J.R., Williams, R.J.P. 2001. The Biological Chemistry of the Elements. Oxford University Press, New York

Gattiker, A., Gasteiger, E., Bairoch, A. 2002. ScanProsite: a reference implementation of a PROSITE scanning tool. *Applied Bioinformatics* **1:**107–108

Gitschier, J., Moffat, B., Reilly, D., Wood, W.I., Fairbrother, W.J. 1998. Solution structure of the fourth metal-binding domain from the Menkes copper-transporting ATPase. *Nat. Struct. Biol.* **5:**47–54

Glynn, I. 1985. The Na^+,K^+-transporting adenosine triphosphatase. *In*: Enzymes of Biological Membranes. Martonosi, A. editor. pp. 35–114. Plenum PL, New York

Herrmann, L., Schwan, D., Garner, R., Mobley, H.L., Haas, R., Schafer, K.P., Melchers, K. 1999. *Helicobacter pylori* cadA encodes an essential Cd(II)-Zn(II)-Co(II) resistance factor influencing urease activity. *Mol. Microbiol.* **33:**524–536

Hirayama, T., Kieber, J.J., Hirayama, N., Kogan, M., Guzman, P., Nourizadeh, S., Alonso, J.M., Dailey, W.P., Dancis, A., Ecker, J.R. 1999. RESPONSIVE-TO-ANTAGONIST1, a Menkes/Wilson disease-related copper transporter, is required for ethylene signaling in *Arabidopsis*. *Cell* **97:**383–393

Huffman, D.L., O'Halloran, T.V. 2000. Energetics of copper trafficking between the Atx1 metallochaperone and the intracellular copper transporter, Ccc2. *J. Biol. Chem.* **275:**18611–18614

Hughes, M.N. 1988. The Inorganic Chemistry of Biological Processes. John Wiley & Sons Ltd., London

Jordan, I.K., Natale, D.A., Koonin, E.V., Galperin, M.Y. 2001. Independent evolution of heavy metal-associated domains in copper chaperones and copper-transporting atpases. *J. Mol. Evol.* **53:**622–633

Kuntzweiler, T.A., Argüello, J.M., Lingrel, J.B. 1996. Asp804 and Asp808 in the transmembrane domain of the Na,K-ATPase alpha subunit are cation coordinating residues. *J. Biol. Chem.* **271:**29682–29687

La Fontaine, S., Firth, S.D., Lockhart, P.J., Brooks, H., Camakaris, J., Mercer, J.F. 1999. Functional analysis of the Menkes protein (MNK) expressed from a cDNA construct. *Adv. Exp. Med. Biol.* **448:**67–82

Lutsenko, S., Kaplan, J.H. 1995. Organization of P-type ATPases: Significance of structural diversity. *Biochemistry* **34:**15607–15613

MacLennan, D.H., Rice, W.J., Odermatt, A., Green, N.M. 1998. Structure-function relationships in the Ca^{2+}-binding and translocation domain of SERCA1: physiological correlates in Body disease. *Acta Physiol. Scand. Suppl.* **643:**55–67

Mandal, A.K., Cheung, W.D., Argüello, J.M. 2002. Characterization of a thermophilic P-type Ag+/Cu+-ATPase from the extremophile *Archaeoglobus fulgidus*. *J. Biol. Chem.* **277:**7201–7208

Melchers, K., Weitzenegger, T., Buhmann, A., Steinhilber, W., Sachs, G., Schofer, K.P. 1996. Cloning and membrane topology of a P type ATPase from *Helicobacter pylori*. *J. Biol. Chem.* **271:**446–457

Mitra, B., Sharma, R. 2001. The cysteine-rich amino-terminal domain of ZntA, a Pb(II)/Zn(II)/Cd(II)-translocating ATPase from *Escherichia coli*, is not essential for its function. *Biochemistry* **40:**7694–7699

Odermatt, A., Suter, H., Krapf, R., Solioz, M. 1993. Primary structure of two P-type ATPases involved in copper homeostasis in *Enterococcus hirae*. *J. Biol. Chem.* **268:**12775–12779

Ogawa, H., Toyoshima, C. 2002. Homology modeling of the cation binding sites of Na^+,K^+-ATPase. *Proc. Natl. Acad. Sci. USA* **99:**15977–15982

Okkeri, J., Haltia, T. 1999. Expression and mutagenesis of ZntA, a zinc-transporting P-type ATPase from *Escherichia coli*. *Biochemistry* **38:**14109–14116

Palmgren, M.G., Axelsen, K.B. 1998. Evolution of P-type ATPases. *Biochim. Biophys. Acta* **1365:**37–45

Paulsen, I.T., Saier, M.H., Jr. 1997. A novel family of ubiquitous heavy metal ion transport proteins. *J. Membrane Biol.* **156:**99–103

Pearson, R.G. 1963. Hard and soft acids and bases. *J. Am. Chem. Soc.* **85:**3533–3539

Pedersen, P.A., Nielsen, J.M., Rasmussen, J.H., Jorgensen, P.L. 1998. Contribution to Tl^+, K^+, and Na^+ binding of Asn776, Ser775, Thr774, Thr772, and Tyr771 in cytoplasmic part of fifth transmembrane segment in alpha-subunit of renal Na,K-ATPase. *Biochemistry* **37:**17818–17827

Pedersen, P.A., Rasmussen, J.H., Nielsen, J.M., Jorgensen, P.L. 1997. Identification of Asp804 and Asp808 as Na^+ and K^+ coordinating residues in alpha-subunit of renal Na,K-ATPase. *FEBS Lett.* **400:**206–210

Pedersen, P.L., Carafoli, E. 1987. Ion motive ATPases: I. Ubiquity, properties, and significance to cell function. *Trends Biochem. Sci.* **12:**146–150

Petris, M.J., Mercer, J.F., Culvenor, J.G., Lockhart, P., Gleeson, P.A., Camakaris, J. 1996. Ligand-regulated transport of the Menkes copper P-type ATPase efflux pump from the Golgi apparatus to the plasma membrane: a novel mechanism of regulated trafficking. *Embo J.* **15:**6084–6095

Petrukhin, K., Lutsenko, S., Chernov, I., Ross, B.M., Kaplan, J.H., Gilliam, T.C. 1994. Characterization of the Wilson disease gene encoding a P-type copper transporting ATPase: genomic organization, alternative splicing, and structure/function predictions. *Hum. Mol. Genet.* **3:**1647–1656

Phung, L.T., Ajlani, G., Haselkorn, R. 1994. P-Type Atpase from the cyanobacterium *Synechococcus*-7942 related to the human Menkes and Wilson disease gene-products. *Proc. Natl. Acad. Sci. USA* **91:**9651–9654

Rensing, C., Fan, B., Sharma, R., Mitra, B., Rosen, B.P. 2000. CopA: An *Escherichia coli* Cu(I)-translocating P-type ATPase. *Proc. Natl. Acad. Sci. USA* **97:**652–656

Rensing, C., Ghosh, M., Rosen, B.P. 1999. Families of soft-metal-ion-transporting ATPases. *J. Bacteriol.* **181:**5891–5897

Rensing, C., Mitra, B., Rosen, B.P. 1997. The zntA gene of *Escherichia coli* encodes a Zn(II)-translocating P-type ATPase. *Proc. Natl. Acad. Sci. USA* **94:**14326–14331

Rensing, C., Sun, Y., Mitra, B., Rosen, B.P. 1998. Pb(II)-translocating P-type ATPases. *J. Biol. Chem.* **273:**32614–32617

Rutherford, J.C., Cavet, J.S., Robinson, N.J. 1999. Cobalt-dependent transcriptional switching by a dual-effector MerR-like protein regulates a cobalt-exporting variant CPx-type ATPase. *J. Biol. Chem.* **274:**25827–25832

Schaefer, M., Hopkins, R.G., Failla, M.L., Gitlin, J.D. 1999. Hepatocyte-specific localization and copper-dependent trafficking of the Wilson's disease protein in the liver. *Am. J. Physiol.* **276:**G639–G646

Sharma, R., Rensing, C., Rosen, B.P., Mitra, B. 2000. The ATP hydrolytic activity of purified ZntA, a Pb(II)/Cd(II)/Zn(II)-translocating ATPase from *Escherichia coli*. *J. Biol. Chem.* **275:**3873–3878

Silver, S., Phung, L.T. 1996. Bacterial heavy metal resistance: new surprises. *Ann. Rev. Microbiol.* **50:**753–789

Solioz, M., Camakaris, J. 1997. Acylphosphate formation by the Menkes copper ATPase. *FEBS Lett.* **412:**165–168

Solioz, M., Odermatt, A. 1995. Copper and silver transport by CopB-ATPase in membrane vesicles of *Enterococcus hirae*. *J. Biol. Chem.* **270:**9217–9221

Solioz, M., Vulpe, C. 1996. CPx-type ATPases: a class of P-type ATPases that pump heavy metals. *Trends Biochem. Sci.* **21:**237–241

Sonnhammer, E.L.L., von Heijne, G., Krogh, A. 1998. A hidden Markov model for predicting transmembrane helices in protein sequences. *In:* Proc. of Sixth Int. Conf. on Intelligent Systems for Molecular Biology. Glasgow, J., Littlejohn, T., Major, F., Lathrop, R., Sankoff, D. and Sensen, C., editors. pp. 175–182. AAAI Press, Menlo Park, CA

Sweadner, K.J., Donnet, C. 2001. Structural similarities of Na,K-ATPase and SERCA, the Ca^{2+}-ATPase of the sarcoplasmic reticulum. *Biochem. J.* **356:**685–704

Thelwell, C., Robinson, N.J., Turner-Cavet, J.S. 1998. An SmtB-like repressor from *Synechocystis* PCC 6803 regulates a zinc exporter. *Proc. Natl. Acad. Sci. USA.* **95:**10728–107033

Thompson, J.D., Higgins, D.G., Gibson, T.J. 1994. CLUSTAL W: improving the sensitivity of progressive multiple sequence alignment through sequence weighting, position-specific gap penalties and weight matrix choice. *Nucleic Acids Res.* **22:**4673–4680

Toyoshima, C., Nakasako, M., Nomura, H., Ogawa, H. 2000. Crystal structure of the calcium pump of sarcoplasmic reticulum at 2.6 Å resolution. *Nature* **405:**647–655

Toyoshima, C., Nomura, H. 2002. Structural changes in the calcium pump accompanying the dissociation of calcium. *Nature* **418:**605–611

Tsai, K.J., Lin, Y.F., Wong, M.D., Yang, H.H., Fu, H.L., Rosen, B.P. 2002. Membrane topology of the p1258 CadA Cd(II)/Pb(II)/Zn(II)-translocating P-type ATPase. *J. Bioenerg. Biomembr.* **34:**147–156

Tsai, K.J., Linet, A.L. 1993. Formation of a phosphorylated enzyme intermediate by the cadA Cd(2+)-ATPase. *Arch. Biochem. Biophys.* **305:**267–270

Tsai, K.J., Yoon, K.P., Lynn, A.R. 1992. ATP-dependent cadmium transport by the cadA cadmium resistance determinant in everted membrane vesicles of *Bacillus subtilis*. *J. Bacteriol.* **174:**116–121

Tsivkovskii, R., MacArthurs, B., Lutsenko, S. 2001. The Lys(1010)-Lys(1325) fragment of the Wilson's disease protein binds nucleotides and interacts with the N-terminal domain of this protein in a copper-dependent manner. *J. Biol. Chem.* **276:**2234–2242

Vilsen, B., Andersen, J.P. 1998. Mutation to the glutamate in the fourth membrane segment of Na^+,K^+-ATPase and Ca^{2+}-ATPase affects cation binding from both sides of the membrane and destabilizes the occluded enzyme forms. *Biochemistry* **37:**10961–10971

Voskoboinik, I., Brooks, H., Smith, S., Shen, P., Camakaris, J. 1998. ATP-dependent copper transport by the Menkes protein in membrane vesicles isolated from cultured Chinese hamster ovary cells. *FEBS Lett.* **435:**178–182

Voskoboinik, I., Mar, J., Strausak, D., Camakaris, J. 2001. The regulation of catalytic activity of the menkes copper-translocating P-type ATPase. Role of high affinity copper-binding sites. *J. Biol. Chem.* **276:**28620–28627

Voskoboinik, I., Strausak, D., Greenough, M., Brooks, H., Petris, M., Smith, S., Mercer, J.F., Camakaris, J. 1999. Functional analysis of the N-terminal CXXC metal-binding motifs in the human Menkes copper-transporting P-type ATPase expressed in cultured mammalian cells. *J. Biol. Chem.* **274:**22008–22012

Vulpe, C.D., Packman, S. 1995. Cellular copper transport. *Ann. Rev. Nutr.* **10:**293–322

Williams, L.E., Pittman, J.K., Hall, J.L. 2000. Emerging mechanisms for heavy metal transport in plants. *Biochim. Biophys. Acta* **1465:**104–126

Woeste, K.E., Kieber, J.J. 2000. A strong loss-of-function mutation in RAN1 results in constitutive activation of the ethylene response pathway as well as a rosette-lethal phenotype. *Plant Cell* **12:**443–455

Yoshimizu, T., Omote, H., Wakabayashi, T., Sambongi, Y., Futai, M. 1998. Essential Cys-Pro-Cys motif of *Caenorhabditis elegans* copper transport ATPase. *Biosci. Biotechnol. Biochem.* **62:**1258–1260

Zhou, Y., Morais-Cabral, J.H., Kaufman, A., MacKinnon, R. 2001. Chemistry of ion coordination and hydration revealed by a K^+ channel-Fab complex at 2.0 A resolution. *Nature* **414:**43–48